River Flow 2010 - Dittrich, Koll, Aberle & Geisenhainer (eds) - © 2010 Bundesanstalt für Wasserbau ISBN 978-3-939230-00-7

Flow-vegetation interaction at a scale of individual plant: a case study of *Ranunculus penicillatus*

Fabio Siniscalchi, Vladimir I. Nikora, Stuart M. Cameron
School of Engineering, University of Aberdeen, Fraser Noble Building, AB24 3UE Aberdeen, Scotland;

R.W. Jay Lacey
Département de génie civil, Université de Sherbrooke; 2500 boul. Université Sherbrooke, J1K 2R1 Québec, Canada;

Andrea Marion
Department of Hydraulic, Maritime, Environmental and Geotechnical Engineering, University of Padova; via Loredan 20, 35131 Padova, Italy;

ABSTRACT: Interactions between submerged aquatic vegetation and turbulent flow occur at multiple scales. In this paper we present some results concerning the scale of a single plant. The aim was to investigate the modifications to the flow due to the presence of the plant as well as to evaluate the mean drag force acting on the plant. Six experiments were completed in a 12 m long and 0.30 m wide flume. The flume bed was fully covered with gravel particles (d_{50} = 8.4 mm) and an aquatic plant (*Ranunculus penicillatus*) was placed and fixed in a section 6.7 m downstream of the flume entrance. In the experiments, the plant consisted of either ten or twenty stems and three different flow scenarios were tested. Velocity vector components were measured at multiple points upstream and downstream of the plants using two Acoustic Doppler Velocimeters (ADV), and estimates of the drag force were obtained by means of the momentum integral method. The results showed that the turbulent energy downstream of the plant was always larger than upstream, and the difference increased with the number of stems and flow velocity. The power spectral density of the downstream velocity revealed modifications of the conventional turbulent scalings. The integral length scale behind the plant was roughly constant in the vertical direction, indicating that the scaling distance for turbulent structures was the distance from the plant rather than from the bed. The estimated mean drag on the plants increased with number of stems and flow velocity.

Keywords: Submerged plant, Turbulence, Open channel, Drag

1 INTRODUCTION

Submerged aquatic plants significantly influence flow structure and therefore have a direct impact on the transport of sediments, nutrients and contaminants. Rooted plants function as a link between sediments in the bed of the channel and the water above, thus they also affect the transport of substances (*e.g.*, nutrients) between these two components of the system (Clarke, 2002).

Interactions between submerged vegetation and turbulent flow act at multiple scales, which are leaf, shoot, plant, plant patch and patch mosaic scales. On one hand, vegetation in flowing water adopts special mechanisms (*e.g.* flapping) to improve its performances, in terms of nutrient uptake and photosynthesis (Nikora, 2009). On the other hand, vegetation modifies sediment transport and flow resistance by changing mixing processes and altering the overall drag force on the bed.

The total drag force can be assumed to be the sum of two components: skin friction and pressure (form) drag (*e.g.*, Massey, 1989). Skin friction is due to the viscous forces exerted at the water-plant surface interfaces. Pressure drag is related to the pressure difference that exists between front and back parts of the object under study, and this difference is often associated with flow separation.

Because of the drag force, aquatic plants require morphological adaptations to prevent mechanical damage and uprooting: such a mechanism is known as 'reconfiguration' (*e.g.*, Vogel, 1984, Sand-Jensen, 2003). In order to minimise the total drag, plants may employ two forms of reconfiguration. First, they tend to 'compress' leaves and stems to each other to achieve a more streamlined overall shape and to reduce the frontal area. Second, at higher flows, plants bend closer to the bed, where velocities are lower, forming a shielding canopy. As a result,

only the upper surface of the plants is subjected to the high flow velocities (Sand-Jensen, 2003).

Vegetation is typically organised in patches. Therefore, many authors have studied the flow within and above vegetated canopies, both terrestrial (Raupach *et al.*, 1996, Finnigan, 2000) and aquatic (Ghisalberti and Nepf, 2002, Poggi *et al.*, 2004). The studies of flow-vegetation interactions at the scale of an individual plant should provide important additional information (*e.g.*, Green, 2005), such as the size of the wake region, the effect on turbulent energy production and other turbulent characteristics.

Therefore, the focus of this paper is on individual plants. The aim of the reported laboratory study was to better understand the impact of single submerged aquatic plants on the flow structure. In §2 we present a general description of the facilities and instruments, the plants and the experimental setup. In §3 we describe the parameters that have been analysed. In §4 we discuss our findings, related to velocity spectra, plant transfer function, integral length scale, and mean values of drag force.

2 EXPERIMENTS

The experiments were conducted in a 12 m long and 0.3 m wide rectangular flume in the Fluid Mechanics Laboratory of the University of Aberdeen (Scotland). In each experiment, flow velocities were measured in different points upstream and downstream of a submerged isolated plant. Before starting the experiments, the bed of the flume was cleaned and then covered with a 2 cm thick gravel (d_{50} = 8.4 mm) layer, in order to develop an appropriate boundary layer on a rough bed representative of natural conditions. The experiments have been conducted at (quasi) uniform flow conditions.

The water depth was set to 0.14 m in each experiment. As width to depth ratio was low, secondary currents were most likely present. However, their presence does not affect the comparisons between the flow upstream and downstream of the plant.

Velocities were measured using two Nortek 10 MHz Acoustic Doppler Velocimeters (ADVs, http://www.nortek-as.com). The sampling volume height was fixed at 0.9 cm and the sampling frequency was set to 50 Hz for all experiments.

Aquatic plants (*Ranunculus penicillatus*) were collected from the Don River in Aberdeen and then used in the experiments (only fresh plants have been studied). Plant material was used to make two plant types, 10 and 20 stem/shoot plants, created by connecting natural shoots together. These semi-artificial plants closely resembled the natural ones. Figure 1 shows a plant during an experiment.

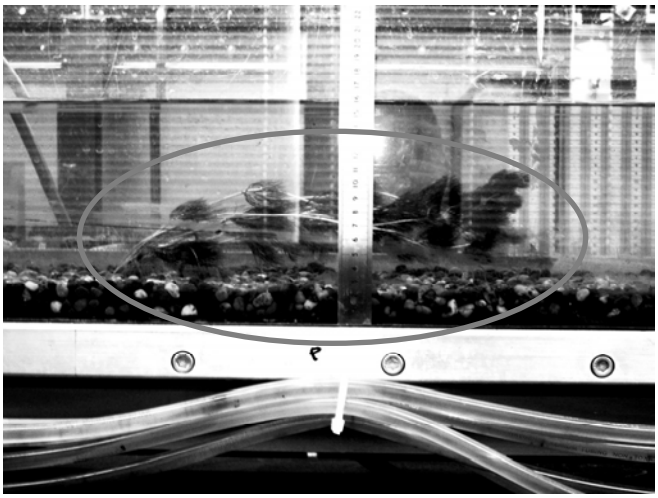

Figure 1. Side view of the plant during the experiment.

Six different experiments were conducted, each one having a particular flow scenario (A, B, or C) and a plant type (10 or 20 shoots). The flow scenarios were chosen from a combination of flow rates and flume slopes (Table 1).

The stems/shoots were cut 40 cm long, tied all together on the base and then fixed to a metal plate. The plate was placed on the bed of the flume and then covered within the gravel layer, so that it did not disturb the flow. The plants were positioned 6.7 m from the entrance of the channel.

The coordinate system adopted here is x for direction parallel to the main flow, y for transverse direction and z for the upward vertical direction. The origin is located on the right wall 6.7 m from the flume entrance, 2 cm above the flume bed (*i.e.*, at the top of the gravel layer, see Figures 2 and 3).

Six measurement sections were chosen at x = -20, 0, 20, 40, 60, 80 cm. In each section, measurements were taken in five verticals and at four elevations (see Figure 3). Both ADVs (named 'probe 0' and 'probe 1') were used simultaneously, and were positioned at the same transverse and vertical coordinates, but at different x-sections. Measurement duration at each point was 120 seconds, which is much longer than the integral time scales of studied turbulent flows.

Table 1. Background parameters of the experiments

Scenario	Flow rate Q (m^3/s)	Slope S_0 (‰)	Water depth H (m)	Mean velocity $U=Q/A$ (m/s)	Fr	Re	u_* (m/s)	Deflected plant height H_p (cm)
A	0.025	2.416	0.140	0.60	0.51	81 922	0.041	5 - 7
B	0.018	1.379	0.140	0.43	0.37	60 828	0.031	6 - 8
C	0.011	0.723	0.140	0.26	0.22	35 503	0.023	8 - 9

Table 1 presents a summary of the background parameters, where $Fr = U/(gH)^{1/2}$ is the global Froude number, $Re = UH/\nu$ is the global Reynolds number, $u_* = (gS_0R_H)^{1/2}$ is the global shear velocity, g is the gravitational acceleration, R_H is the hydraulic radius.

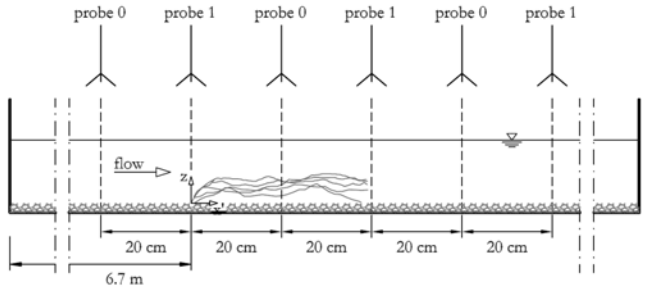

Figure 2. Side view of the experimental setup.

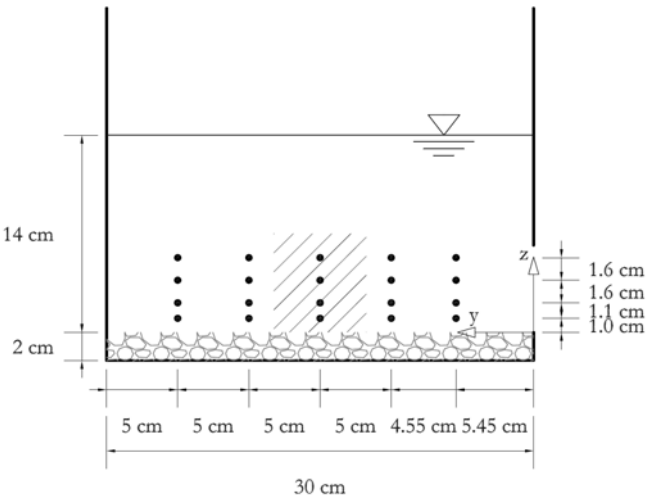

Figure 3. Cross section showing the points of measurements. The oblique lines indicate the area occupied by the plant.

3 ANALYSES

Several parameters were analysed in order to characterise plant-flow interactions.

The power spectral density function (PSD) of a velocity time series is an important parameter because it is related to the turbulent energy of the flow. It can be calculated as a Fourier transform of the correlation function, $R_{ii}(\tau)$, and generally it is defined over nonnegative frequencies (one-sided spectrum):

$$G_{ii}(f) = 2S_{ii}(f) = 2\int_{-\infty}^{+\infty} R_{ii}(\tau)e^{-j2\pi f\tau}\,d\tau \quad (1)$$

where S_{ii} is the two-sided spectrum and f is the signal frequency. The comparison of turbulent energy upstream and downstream of the plant was made using the measurements taken at the flume centreline (y = 15 cm).

The plant transfer function (PTF) is a parameter that links output and input signals in the frequency domain. In the present study, it provides information about turbulent energy variations owing to the plant. PTF is evaluated as:

$$H^2_{plant}(f) = \frac{G_{ii,back}(f)}{G_{ii,front}(f)} \quad (2)$$

where $G_{ii,back}$ and $G_{ii,front}$ are the PSD measured downstream and upstream of the plant respectively, at the same elevation z.

The integral length scale (ILS) provides an estimate of the characteristic size of turbulent eddies. It allows comparison of the representative length scales of eddies upstream and downstream of the plant. In order to evaluate ILS, the velocity autocorrelation function is first calculated:

$$R_{ii}(\tau) = \lim_{T\to\infty}\frac{1}{T}\int_0^T u_i(t)u_i(t+\tau)dt \quad (3)$$

where T is the averaging time period and u_i is the velocity component. This function describes the autocorrelation of velocity signals. The integral time scale is then evaluated as:

$$T_i = \int_0^{\infty} R_{ii}(\tau)d\tau \quad (4)$$

Assuming Taylor's frozen turbulence hypothesis, ILS is evaluated as:

$$L_i = u_c T_i \quad (5)$$

where u_c is the eddy convection velocity. Such a velocity can be calculated as a ratio of the distance between the ADVs to the time lag of the peak of the cross-correlation function between the velocity time series:

$$u_c = \frac{D_{probes}}{\tau_{\max}} \quad (6)$$

In order to have a better understanding of the interactions between aquatic plants and flow turbulence, the mean drag force acting on *Ranunculus* was also estimated.

Based on the availability of velocity measurements upstream and downstream of the plants, it was possible to apply the integral momentum equation and evaluate the drag force using a momentum deficit. The resultant force of the external forces exerted by a solid body on a fluid volume in a certain direction equals to the total rate of change of momentum of fluid in that direction (*e.g.*, Massey, 1989). The resultant force exerted on the fluid control volume is equal and opposite to the hydrodynamic force exerted by the fluid on the body.

We can define a control volume such that the outer boundary is formed by the two walls of the flume, the cross-sections at x = -20 cm and x = 60 cm, the top of the gravel layer and a plane placed at z = 5.3 cm parallel to the flume bed. The inner boundary of the control volume is presented by the plant surface. The integral momentum equation (x-component) applied to such a control volume has a form:

$$\int_{x=60} \rho u^2 dA - \int_{x=-20} \rho u^2 dA + \int_{z=5.3} \rho wu dA = \\ = \Delta p + \int_V \rho g_x dV - \int_{bottom+walls} \tau_0 dA - F \quad (7)$$

where Δp is the difference of pressure between upstream and downstream cross-sections, V is the control volume, g_x is the x-component of the gravitational acceleration, τ_0 represents the shear stresses on the bottom and on the walls, F is the plant drag force. We can reasonably assume that the momentum flux through the top boundary is much lower than the other contributors and thus we can neglect it. The gravitational force exactly balances the frictional resistance force. Given that the downstream boundary of the control volume is sufficiently distanced from the plant, we can assume that the difference of pressure between upstream and downstream sections is negligible. Therefore, we obtain:

$$F = \int_{x=-20} \rho u^2 dA - \int_{x=60} \rho u^2 dA \quad (8)$$

Equation 8 was solved numerically:

$$F \cong \rho \sum_j \left(u^2_{j,front} - u^2_{j,back} \right) \Delta y \Delta z \quad (9)$$

where subscript j identifies the measurement points (j = 1, 2,.., 20), Δy and Δz are the sizes of the spatial cells associated with each measurement point, $u_{j,front}$ refers to the local velocity in section x = -20 cm and $u_{j,back}$ refers to section x = 60 cm.

4 RESULTS AND DISCUSSION

An example of the upstream u-, v-, w-velocity spectra is shown in Figure 4.

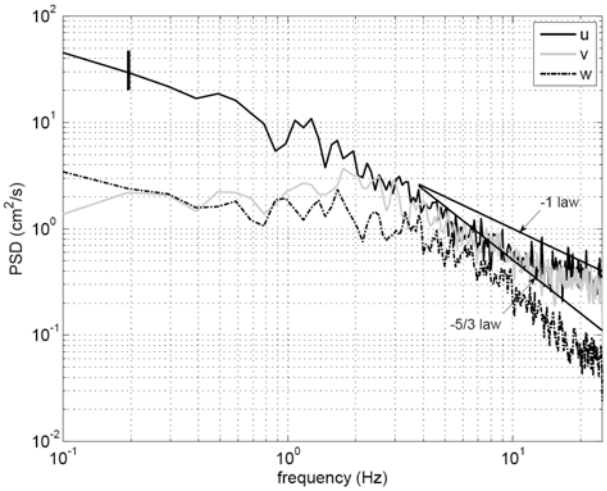

Figure 4. Power spectral density of velocity components (Scenario A, 10-stem plant, x= -20 cm, y= 10 cm, z= 5.3 cm); the vertical bar indicates the 95% confidence interval.

Figures 5 and 6 show the w-spectra calculated in the upstream (x = -20 cm, y = 15 cm, z= 5.3 cm) and downstream (x = 60 cm, y = 15 cm, z = 5.3 cm) positions, for Scenario A, with a 10-stem plant. The w-spectra are presented as, due to ADV probe geometry, the w component is much less affected by Doppler noise than the u or v components (Nikora and Goring, 1998) and therefore trends in the power spectra can more readily be discerned.

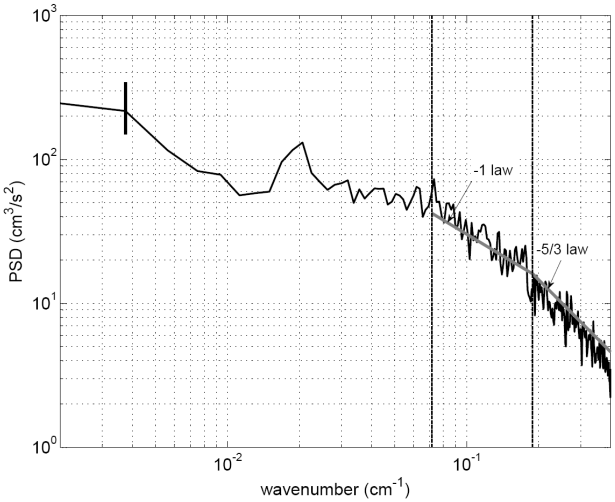

Figure 5. PSD of w-velocity upstream of the plant (Scenario A, 10-stem plant, x= -20 cm, y= 15 cm, z= 5.3 cm); the vertical bar indicates the 95% confidence interval.

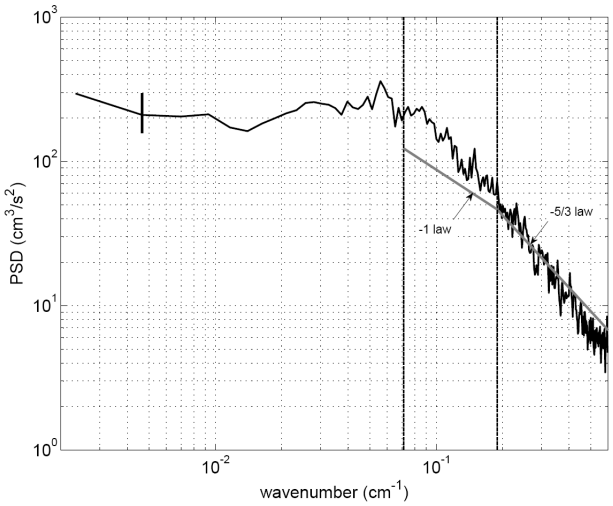

Figure 6. PSD of *w*-velocity downstream of the plant (Scenario A, 10-stem plant, *x*= 60 cm, *y*= 15 cm, *z*= 5.3 cm); the vertical bar indicates the 95% confidence interval.

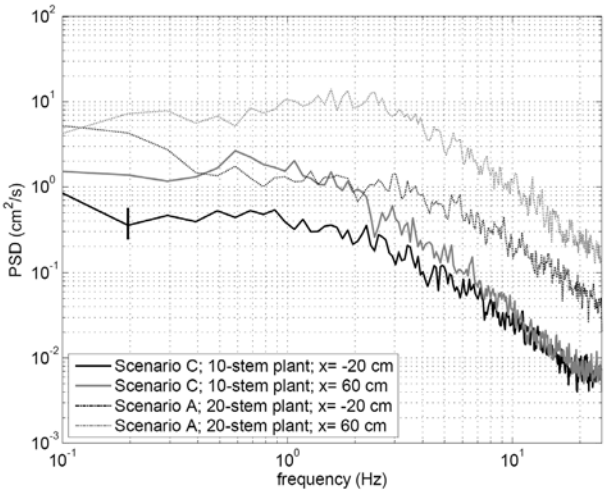

Figure 7. Comparison between PSD of *w*-velocity upstream and downstream of the plant (*y*= 15 cm; *z* = 5.3 cm); the vertical bar indicates the 95% confidence interval.

Figure 7 presents comparisons between spectra in relation to flow scenarios and number of stems of the plants.

Velocity spectra show that turbulent energy downstream of the plant is greater than upstream. Energy spectra related to back positions generally plotted above spectra related to front positions, and this difference increases with flow rate and number of stems (Figure7). Results also show that difference in energy increases with increasing vertical position, *i.e.* downstream turbulent energy enhances away from the bed. Furthermore, in most spectra downstream of the plant it is possible to notice an energy increase within the frequency range $5 \cdot 10^{-1}$ to $3 \cdot 10^{0}$ Hz. This is likely due to wake production caused by plant shoots.

Velocity spectra can be divided in four ranges: the low-frequency production range, the intermediate range where spectrum follows the "-1" law, the inertial subrange with Kolmogorov's "-5/3" law, and the viscous dissipative range (*e.g*, Nikora, 2005). The "-1" law applies in the wavenumber range $1/\alpha_1 H \leq k \leq 1/\alpha_2 z$, where, α_1 and α_2 are scale coefficients, k is the wavenumber, H is the external scale of the flow (*i.e.*, depth), z is the distance of a measurement point from the wall. The "-5/3" law applies for $k \geq 1/\alpha_2 z$. In most spectra upstream of the plant these ranges are observable (Figure 5), demonstrating the general accuracy of measurements. In spectra obtained downstream of the plant such ranges are not clearly observed, suggesting that the plant modifies the spectral structure of turbulence (Figure 6). Flow characteristics downstream are modified by the plant and H and z scales likely lose their significance. In these cases, the characteristic scales should probably be related to plant geometry.

Figure 8 shows H^2_{plant} related to x = -20 cm and x = 60 cm (y = 15 cm, z = 5.3 cm, Scenario A, 10-stem plant). Figure 9 presents H^2_{plant} related to the same experiment and locations, but at an elevation closer to the gravel bed (z = 1 cm).

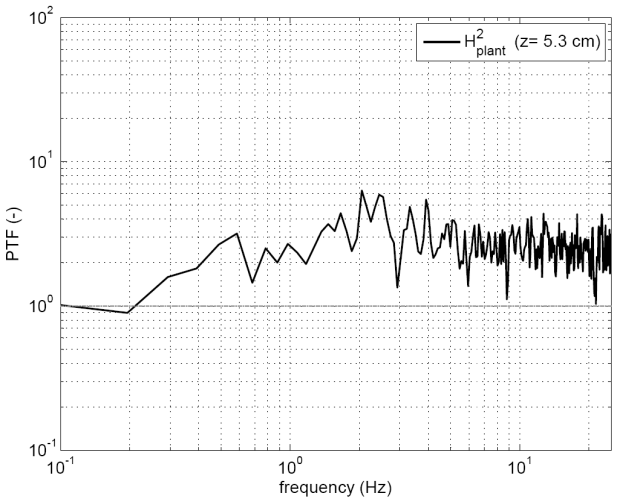

Figure 8. Plant transfer function (dimensionless) related to PSD of *u*-velocity (*z*= 5.3 cm).

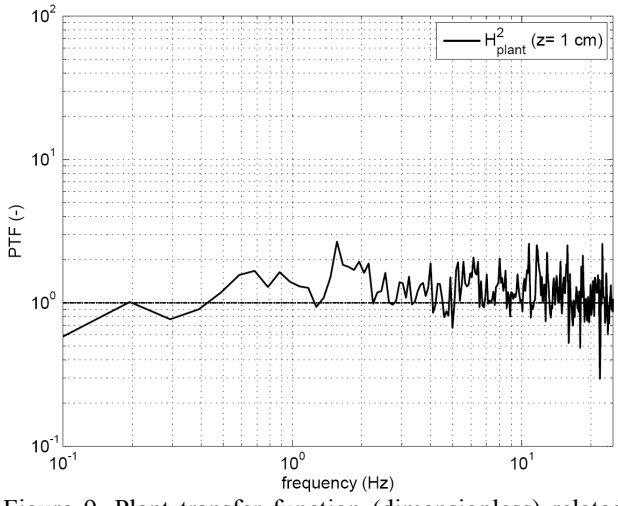

Figure 9. Plant transfer function (dimensionless) related to PSD of *u*-velocity (*z* = 1 cm).

Plant transfer function describes how plant alters turbulent energy at different scales. In most cases,

this parameter is greater than 1, confirming that plants increase the turbulent energy. It is noticed that H^2_{plant} increases with frequency in the range 10^{-1} Hz < f < $1 \cdot 10^{0}$ Hz. At high frequencies (above 1 Hz) H^2_{plant} tends to decrease towards 1 or to fluctuate around a constant value, likely because of an increase in relative noise. Plants do not exhibit a significant influence on the flow turbulent energy at low elevations, near the gravel bed, for which H^2_{plant} is closer to unity at all frequencies (Figure 9). At the lowest flow (Scenario C), the plants do not change eddy energy significantly. This is confirmed also by an extremely low value of the drag force (Table 2). This quite peculiar effect is the result of a combination of a relatively low flow velocity and a highly flexible plant capable of reconfiguring its geometry to minimise its 'visibility' to the flow.

Figure 10 presents a comparison among ILS at the centreline of the flume (y = 15 cm) at three different sections (x = -20 cm, x = 60 cm, x = 80 cm), based on the longitudinal velocity component (Scenario B, 20-stem plant).

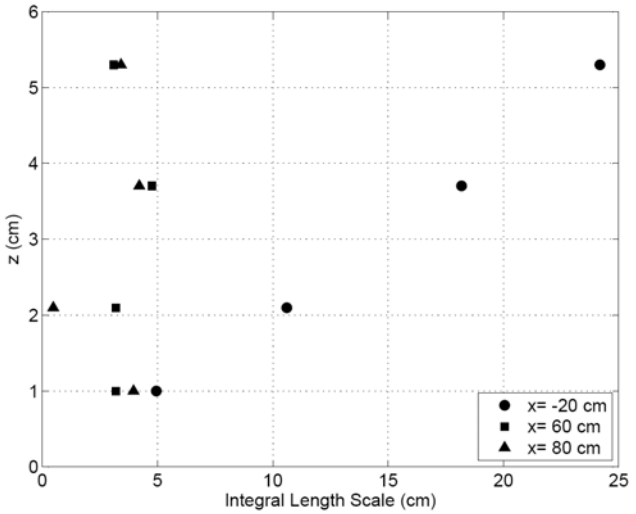

Figure 10. Integral length scale evaluated at three different sections at the flume centreline (y = 15 cm), based on the longitudinal velocity component (Scenario B, 20-stem plant).

Results show that the integral length scale, analysed at the flume centreline, is generally larger upstream of the plant, *i.e.* downstream turbulence is due to smaller eddies, most likely generated by the fluctuating stems and leaves. The mean dimension of upstream eddies increases with the distance from the bed, as one would expect (Figure 10). This trend disappears downstream of the plant, which interacts with the flow by modifying eddy structure. The ILS downstream of the plant is no longer a function of the distance from the bed, and it is rather constant in the vertical direction. This is explained by the fact that the scaling distance for the turbulent structures is the distance from the plant rather than from the bed. This behaviour is reproduced very clearly in all experiments (see Siniscalchi, 2008, for the full set of data).

Table 2 presents the results of the drag estimation.

Table 2. Mean drag forces acting on the plants

Scenario	Drag force ($N \times 10^{-2}$)	
	10 stems	20 stems
A	13.40	14.56
B	10.12	22.24
C	1.51	3.93

Plants withstood drag forces by means of reconfiguration: they bend and streamline with increase in velocity. The mean drag force acting on the plants is expected to increase with the flow rate and the number of stems/shoots. The results verify this hypothesis for most of experiments. Only in one case drag is higher at Scenario B than at Scenario A (20-stem plant). The method adopted for evaluating mean drag forces acting on plants involves some uncertainties related to the measurement coverage of the sections. Data were collected only in a limited part of each section (see Figure 3), thus the control volume was restricted to this area. However, during the experiments, plants could rise towards the water surface and cross the upper boundary of the control volume, leading to wrong evaluation of the drag forces. Nevertheless, such a method is potentially important and fruitful and needs a validation with direct force measurements.

5 CONCLUSIONS

This paper presents results on the interactions between turbulent flow and isolated aquatic plants. The analyses included velocity spectra, plant transfer functions, integral length scales, as well as the evaluation of mean drag forces acting on the plants.

It was shown that turbulent energy is always higher downstream of the plant than upstream and this effect was noted to be stronger with increasing flow velocity and number of stems. The integral length scale is modified downstream of the plant, and it appears to be roughly constant in the vertical direction. Therefore, the scaling for the turbulent structure lengths seems to be related to the distance from the plant rather than from the flume bed.

The technique for evaluating the mean drag force acting on the single plant produced

reasonable results, as the force values reflected flow velocity and number of stems of the plant. In one case, however, the drag estimate appeared to be unreasonable, suggesting that the method has to be improved by considering the entire flow depth for the control volume.

ACKNOWLEDGEMENTS

The work was partly supported by the Leverhulme Trust, Grant F/00152/Z 'Biophysics of flow-plant interactions in aquatic systems' and the Socrates-Erasmus Programme.

NOTATION

The following symbols are used in this paper:

A	control section for the evaluation of drag force;
d_{50}	size of particle mean-axis for which 50% is finer;
D_{probes}	distance between the ADVs;
F	mean drag force;
f	frequency of velocity signal;
Fr	global Froude number;
g	gravitational acceleration;
g_x	x-component of the gravitational acceleration;
$G_{ii}(f)$	velocity autospectrum (one-sided);
$G_{ii,back}$	velocity autospectrum evaluated downstream of the plant;
$G_{ii,front}$	velocity autospectrum evaluated upstream of the plant;
H	water depth;
H_p	deflected plant height;
H^2_{plant}	Plant transfer function;
k	wavenumber;
L_i	Integral length scale;
Q	flow rate;
Re	global Reynolds number;
$R_{ii}(\tau)$	autocorrelation function;
R_H	hydraulic radius;
S_0	bed slope;
$S_{ii}(f)$	velocity autospectrum (two-sided);
T	averaging time period;
T_i	Integral time scale;
U	mean flow velocity;
V	control volume;
$u(t)$	local velocity in the longitudinal direction;
u_c	convection velocity;
$u_{j,back}$	local longitudinal velocity related to measurement point j at x = 60 cm;
$u_{j,front}$	local longitudinal velocity related to measurement point j at x = -20 cm;
u_*	global shear velocity;
$v(t)$	local velocity in the transverse direction;
$w(t)$	local velocity in the vertical direction;
x, y, z	coordinate axes;
α_1, α_2	scale coefficients;
Δp	difference of pressure
$\Delta y, \Delta z$	sizes of the spatial cells associated with each point of measurement;
ν	kinematic viscosity;
ρ	water density;
τ_0	shear stress;
τ_{max}	time lag obtained from the cross-correlation function.

REFERENCES

Clarke, S.J. (2002). Vegetation growth in rivers: influences upon sediment and nutrient dynamics. Progress in Physical Geography, 26, 159-172.

Finnigan, J. (2000). Turbulence in plant canopies. Annual Review of Fluid Mechanics, 32, 519-571.

Ghisalberti, M., Nepf, H.M. (2002). Mixing layers and coherent structures in vegetated aquatic flows. Journal of Geophysical Research, 170(2), 3.1-3.11.

Green, J. C. (2005). Velocity and turbulence distribution around lotic macrophytes. Aquatic Ecology, 39(1), 1-10.

Massey, B. S. (1989). Mechanics of fluids. 6th edition, Van Nostrand Reinhold.

Nikora, V. (2005). Flow turbulence over mobile gravel-bed: spectral scaling and coherent structures. Acta Geophysica, 53(4), 539-552.

Nikora, V. (2009). Hydrodynamics of aquatic ecosystems: an interface between ecology, biomechanics and environmental fluid mechanics. River Research and Applications, DOI: 10.1002/rra.1291.

Nikora, V., Goring, D. (1998). ADV measurements of turbulence: can we improve their interpretation? Journal of Hydraulic Engineering, 124(6), 630-634.

Poggi, D., Porporato, A., Ridolfi, L., Albertson, J.D., Katul, G.G. (2004). The effect of vegetation density on canopy sublayer turbulence. Boundary-Layer Meteorology, 111, 565-587.

Raupach, M.R., Finnigan, J.J., Brunet, Y. (1996). Coherent eddies and turbulence in vegetation canopies: the mixing-layer analogy. Boundary-Layer Meteorology, 78, 351-382.

Sand-Jensen, K. (2003). Drag and reconfiguration of freshwater macrophytes. Freshwater Biology, 48, 271-283.

Siniscalchi, F. (2008). Aquatic plant-turbulence interactions in an open-channel flow: an experimental study. Master's Thesis, Università degli Studi di Padova, Italy.

Vogel, S. (1984). Drag and flexibility in sessile organisms. American Zoology, 24, 37-44.